EXPERIMENTAL STUDY ON STEEL ELLIPTICAL HOLLOW SECTION UNDER AXIAL COMPRESSION

[1]Vinodh Kumar Balaji and [2]T.udaya Kumar Reddy
[1] Associate Professor, [2]PG Student
[1,2]Department of Civil Engineering
[1,2]Siddharth Institute of Engineering & Technology, Puttur, India

Abstract- Elliptical hollow sections represent the recent addition to the range of tubular structural products. Their distinct closed nature brings structural efficiency by offering differing flexural rigidities about each of the principal axes as well as high torsional stiffness. It also offers an interesting and unusual smooth streamlined appearance which can be utilised to fulfil contemporary design visions. The varying radius of curvature around the circumference characterises the distinctive structural behaviour of EHS from other tubular sections. In this study, the manifestation of local buckling under compression and in-plane bending about each of the principal axes has been examined, and a system of cross-section classification has been proposed. Plastic shear area formulations have been derived to codify shear resistance along each of the principal axes. Design expressions for combined shear and bending have also been developed to account for the degradation effect on moment resistance with increasing shear. Member column buckling curves have been proposed in accordance with the major steel design standards, including Eurocode 3.
The key components of this research are laboratory testing, numerical modelling and the development of design guidance. A comprehensive experimental programme was performed in order to gather the basic structural performance data at both cross-section and member levels. At cross-section level, a total of 4 tensile coupon tests, 4 stub column tests, 8 in-plane bending tests and 4 shear tests were conducted, whilst at member level, a total of 4 column tests were carried out. At each phase, the experimental results were utilised to validate finite element models, after which parametric studies based upon the validated models were conducted.

Keywords: Elliptical hollow section column, Euro code 3, finite element analysis.

I. INTRODUCTION

This chapter focuses on the compressive resistance of elliptical hollow sections, and provides the results of 4 stub column tests and extensive numerical results. The experimental study included 4 material tensile coupon tests extracted from the tested cross-sections together with geometric imperfection measurements. All tested elliptical hollow sections had an aspect ratio of 2 and section sizes ranged from 150x75 mm. The generated structural performance data have been used to establish association between cross-section slenderness and cross-section compressive resistance and to develop cross-section classification limits.
The distinct feature of an elliptical hollow section from other tubular sections is its varying radius of curvature around the circumference. This varies from a minimum r_{min}=b2/a at the ends of the cross-section minor (z-z) axis to a maximum r_{max}=a2/b at the ends of cross-section major (y-y) axis as shown in Figure 1. The associated stiffness of each constituent segment depends upon its corresponding radius of curvature.
The sum of these segments characterises the overall compressive response of the cross-section, as given by Equation 2.1.

$$N= \int_0^{PM} \sigma c t dPm \qquad (2.1)$$

where N is the axial load, σ_c, is the axial compressive stress, and t and Pm are the thickness and mean perimeter of the cross-section, respectively. Equation 3.1 allows for variation of axial compressive stress around the cross-section with the stiffer parts attracting more load. As described in Section 3.4, the test and numerical results indicate that stocky elliptical hollow sections offer greater load carrying capacity in comparison to their circular counterparts, due to the achievement of strain hardening in the stiffer regions of the section of low radii of curvature.

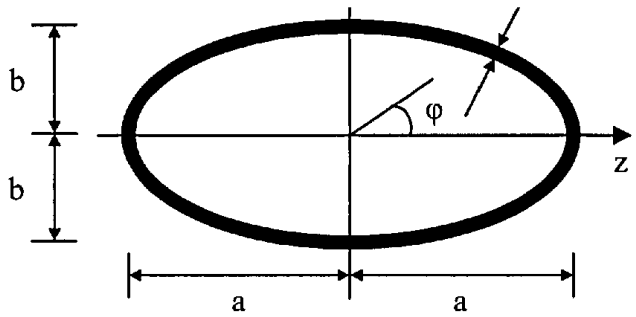

figure 1: geometry of an elliptical hollow section

II. EXPERIMENTAL STUDY

A series of precise full-scale laboratory tests on EHS was performed. The first series of tests comprised a total of 4 material tensile coupon tests and 4 cross-section capacity stub column tests.

Tensile Coupon Tests

The primary objective of the tensile coupon tests was to determine the basic engineering stress-strain behaviour of the material for each of the tested section sizes in this research Results were used to facilitate the numerical study described in Section 3.3 and the development of cross-section classification limits in Section 3.4. Tests were carried out in accordance with EN 10002-1 (2001). Parallel coupons, each with the nominal dimensions of 360x30 mm or 320x20 mm, depending on section size, were machined longitudinally along the centreline of the flattest portions of each of the tested elliptical hollow sections. All tensile tests were performed using a Universal testing machine. To ensure no slippage of the coupons in the jaws of the testing machine, pins were inserted into reamed holes located 20 mm from each end of the coupons.

Linear electrical strain gauges were affixed at the midpoint of each side of the tensile coupons and a series of overlapping proportional gauge lengths was marked onto the surface of the coupons to determine the elongation parameters Mean measured dimensions and the key results from the 4 tensile coupon tests are reported in Table 3.1.

Stub Column Tests

Stub column tests were conducted to develop a relationship between cross-section slenderness, deformation capacity and load-carrying capacity for elliptical hollow sections under uniform axial compression. A total of 4 stub column tests were performed. Full load-end shortening histories were recorded, including into the post-ultimate range. The nominal length of the stub columns was two times the larger outer diameter (2x2a = 4a) of the cross-section. This was deemed sufficiently long to ensure that the stub columns contained a representative distribution of geometric imperfections and residual stresses and to minimise the influence of the end conditions, but suitably short to avoid overall column buckling. The ends of the tubes were milled flat and square. Four linear variable displacement transducers (LVDTs) were located between the parallel end-platens of the testing machine to determine the average end shortening of the stub columns. Four linear electrical resistance strain gauges were affixed to each specimen at mid-height, and at a distance of five times the material thickness from the ends of cross-section minor axis. The strain gauges were initially used for alignment purposes.

The testing arrangement is shown in Figure 2. Load, strain, displacement, and input voltage were all recorded using the data acquisition equipment DATASCAN and logged using the DALITE and DSLOG computer packages. The mean measured dimensions of the stub columns are summarised in Table 3.2. The cross-section area A was calculated from Equation 3.2

$$A=P_m x t \qquad (3.2)$$

table 3.1: mean measured dimensions and key results from the tensile coupon tests

Coupons	Width btc (mm)	Thickness t (mm)	Young's modulus E (N/mm2)	Yield stress fy (N/mm2)	Ultimate tensile stress ft (N/mm2)
150x75x4.0	19.99	4.15	217400	380	512
150x75x5.0	20.15	5.08	217200	364	503
150x75x6.3	19.93	6.36	215200	400	515
150x75x8.0	29.97	8.30	209500	369	502

where Pm is the mean perimeter and t is the thickness of the elliptical hollow section. The exact mean perimeter Pm can be obtained by integrating around the circumference of the ellipse to give Equation 3.3.

$$Pm=4am\int_0^{\frac{\pi}{2}}\sqrt{sin\phi^2+\frac{bm^2}{am^2}cos\phi}\,d\phi \qquad (3.3)$$

in which $a_m = (2a - t)/2$, $b_m = (2b - t)/2$ and φis the angle for each element measured from the z-z axis, as shown in Figure 3.1.

$$P_m = \pi(a_m + b_m)\left(1+\frac{3hm}{10+\sqrt{4-3hm}}\right) \qquad (3.4)$$

For an aspect ratio, a/b of 2, the deviation of Equation 3.4 from the exact solution of Equation 3.3 is only -0.02%. However, as the aspect ratio increases, the maximum deviation increases up to -1.8%. However, consistently underestimates the cross-section area of an EHS with constant thickness due to the implicit non-uniform thickness distribution inherent in the formulation. For example, for a typical EHS of dimensions 2a = 400 mm, 2b = 200 mm and t = 10 mm, Equation 3.2 yields A = 9384 mm2. For accuracy, it is therefore recommended that Equations 3.2 and 3.4 be adopted for the determination of the cross-section area of an EHS, and this approach has been used throughout this research

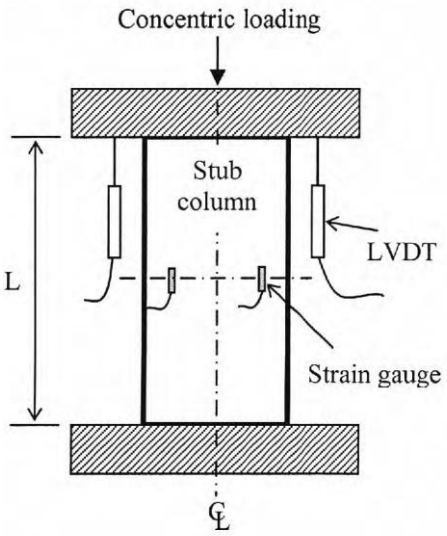

Figure 2: Stub column test arrangement

Table 3.2: Mean measured dimensions of stub column specimens

Stub columns	Larger outer diameter **2a** (mm)	Smaller outer diameter **2b** (mm)	Thickness **t** (mm)	Area **A** (mm2)	Length **L** (mm)	Measured maximum local imperfection $\mathbf{w_o}$ (mm)
150x75x4.0	150.44	75.6	4.18	1471	300	0.04
150x75x5.0	150.17	75.8	5.08	1775	300	0.05
150 x75 x6.3	148.66	75.98	6.27	2150	300	0.04
150 x75 x8.0	150.11	75.1	8.66	2920	300	1.75

Initial geometric imperfection was traced by employing mechanical dial gauge indicator running along the centrelines of the faces of the stub column specimens. The measurement is corrected with reference to the datum taken as a straight line connecting the ends of each stub column face. The primary aim of this exercise was to record the maximum amplitudes of imperfections inherent in hot-finished elliptical tubes; information on the form of the imperfections was also traced. The maximum amplitude of imperfection for each tested specimen is reported in Table 3.2. The full load-end shortening histories from the stub column tests were recorded and are depicted in Figures 3.4 to 3.7. The key results from the stub column tests have been summarised in Table 3.3 where the ultimate test load Nu has been normalised by the yield load Ny = Afy. Values for the ratio Nu/Ny of greater than unity indicate that the cross-sections are capable of reaching the yield load. For slender sections, however, this ratio may be less than unity due to local buckling in the elastic material range.

For sections where Nu/Ny is greater than unity, two patterns of load-end shortening histories were observed. Moderately stocky sections reach and maintain the yield load (along the plastic yield plateau) before failing by inelastic local buckling, examples for very stocky sections, as shown in Figures 3.5, 3.6, and 3.7, the load-end shortening behaviour enters the material strain-hardening regime before local buckling occurs, resulting in ultimate loads greater than the yield load. The full load-end shortening response of the stockiest elliptical hollow sections may be best explained with reference to Figure 3.7, which shows the results for the 150x 75 x8.0 stub columns. The load-end shortening curves may be considered as four regions (labelled 1 to 4 in Figure 3.7). The first region is the elastic loading path which is controlled by the Young's modulus of the material. The second region is the plastic yield plateau which is related to the yield plateau of the material, with the intersection between regions 1 and 2 corresponding to the yield load Ny. The third region reflects the strain-hardening of the material and extends up to the ultimate load Nu, whereupon inelastic local buckling prevents any further increase in load carrying capacity. Region 4 represents the unloading path of the stub columns where growth of local buckles and spreading of plasticity occur.

Table 3.3 Summary of the results from the stub column test

Stub columns	Ultimate load Nu (kN)	End shortening at Nu, δ (mm)	Nu/Ny
150x75x4.0	536	0.5	0.97
150x75x5.0	685	0.7	1.05
150x75x6.3	892	9.7	1.07
150x75x8.0	1362	18.2	1.24

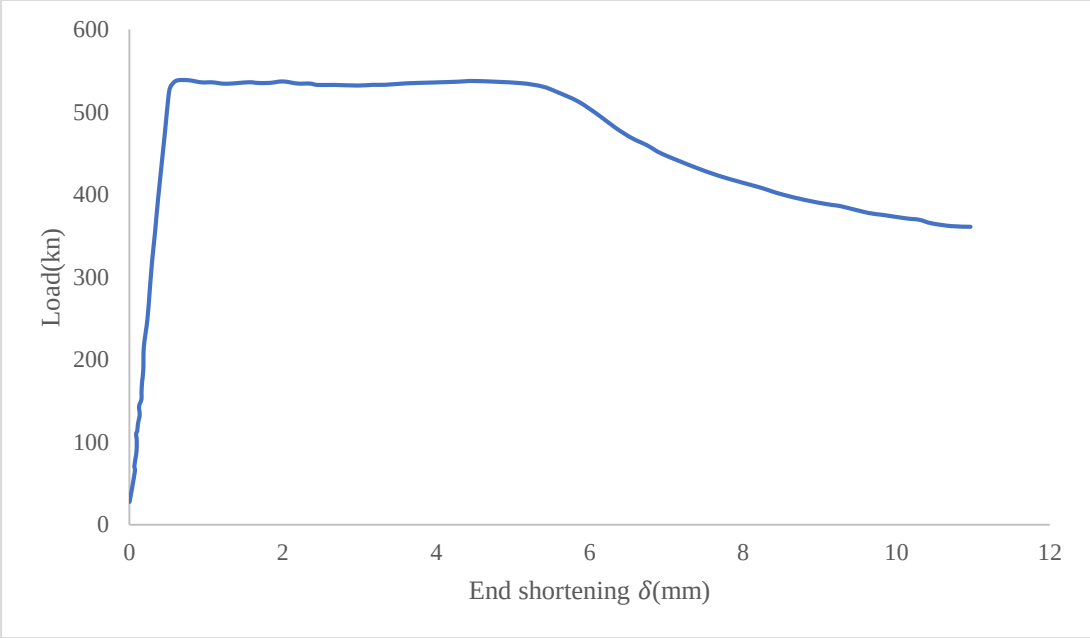

figure 3.4 150 x 75 x 4.0 stub column load-end shortening curves

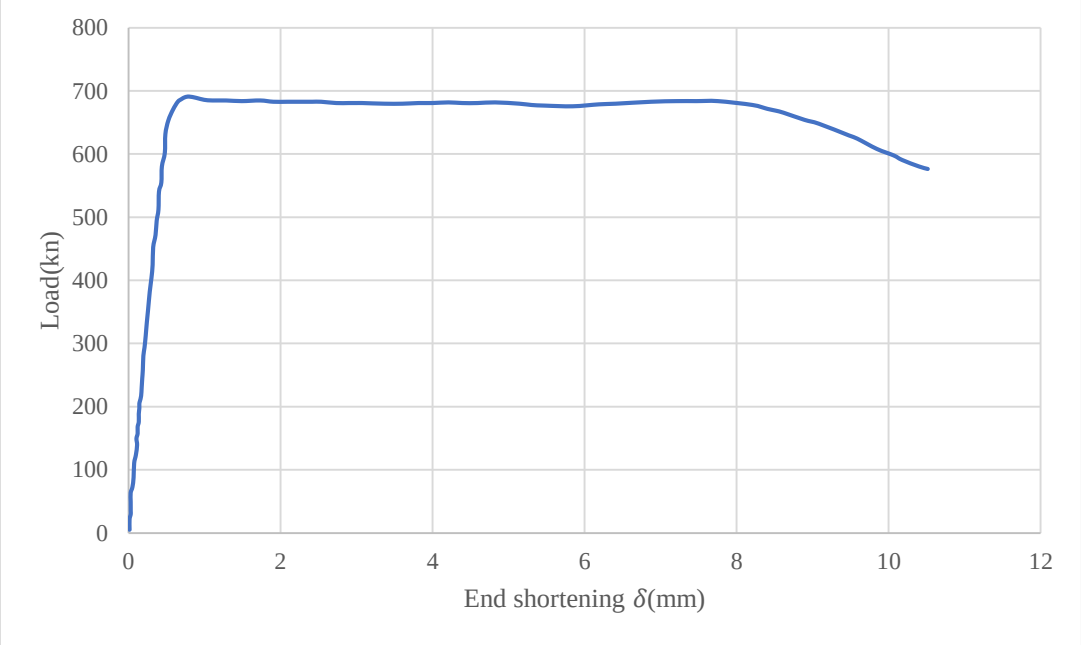

figure 3.5 150 x 75 x 5.0 stub column load-end shortening curves

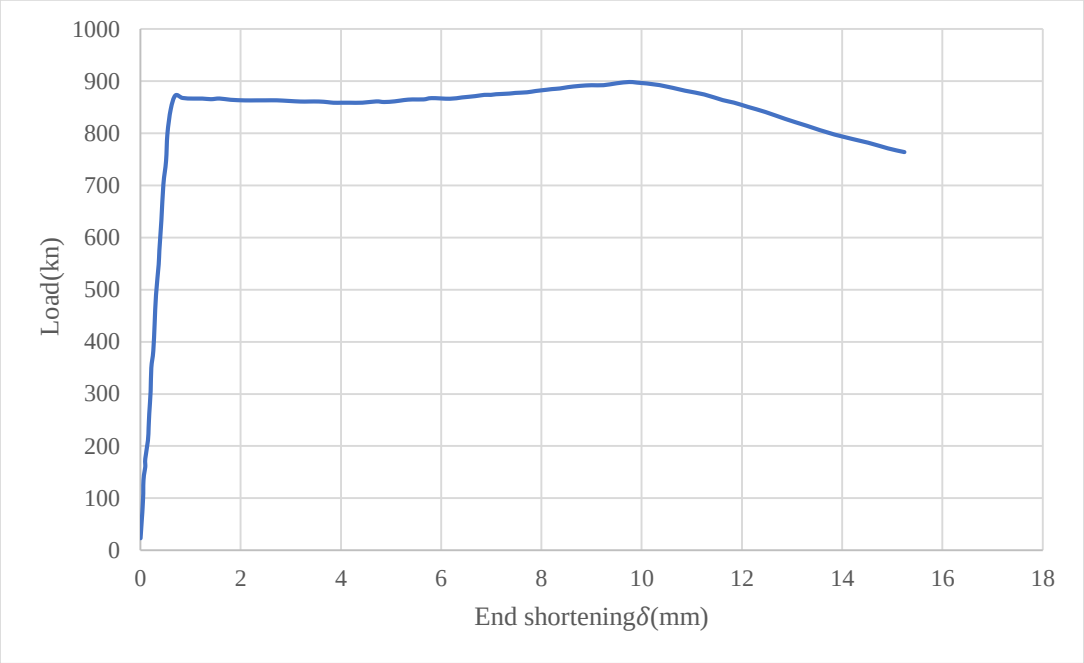

figure 3.6 150x 75 x 6.3 stub column load-end shortening curves

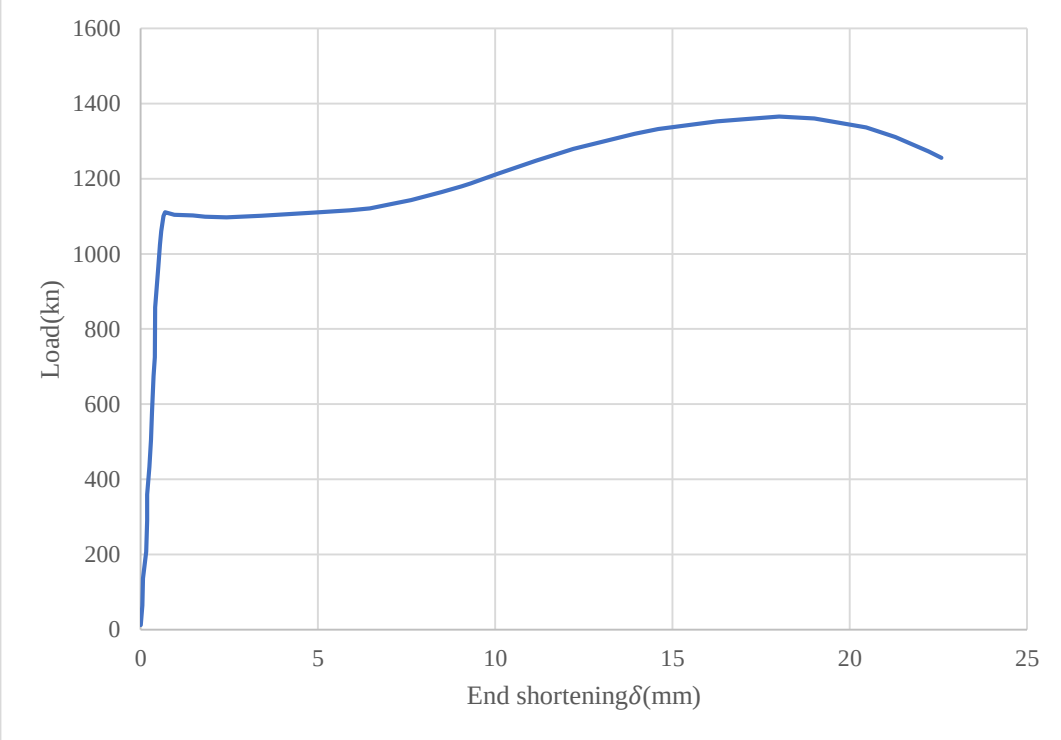

figure 3.7 150x 75 x 8.0 stub column load-end shortening curves

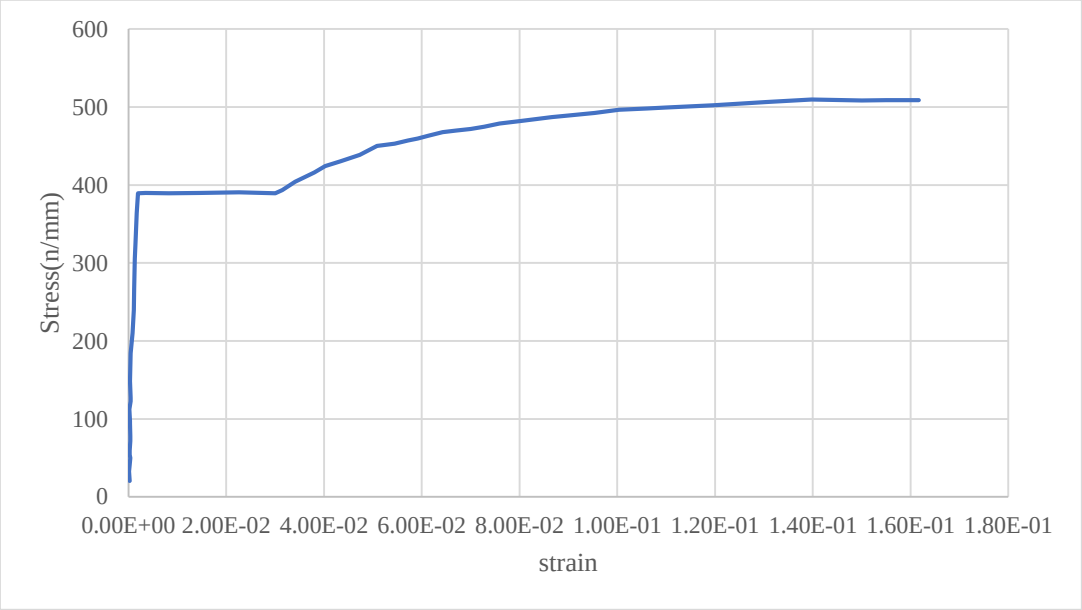

figure 3.8 piecewise linear stress-strain model

III.CONCLUSIONS

In view of the current lack of available design guidance for structural elliptical hollow sections, a series of laboratory tests have been performed. The first series of tests in the experimental programme comprised a total of 4 tensile coupon tests and 4 stub column tests. Results, including geometric imperfection measurements and full load-end shortening curves have been presented.
The resulting structural performance data have been used to establish a relationship between cross-section slenderness and cross-section compressive resistance, which demonstrates that the Class 3 slenderness limit of 90 from Eurocode 3 for circular hollow sections can be safely adopted for elliptical hollow sections based upon the cross-section slenderness parameters proposed in this research and by Ruiz-Teran and Gardner (submitted) with the latter yielding more efficient design.

REFERENCES

[1]. Chan, T. M. and Gardner, L. (in press). Compressive resistance of hot-rolled elliptical hollow sections. *Engineering Structures.*
[2]. Chan, T. M. and Gardner, L. (submitted-a). Bending strength of hot-rolled elliptical hollow sections. *Journal of Constructional Steel Research.*
[3]. Chan, T. M. and Gardner, L. (submitted-b). Flexural buckling of elliptical hollow section columns. *Journal of Structural Engineering*, ASCE.
[4]. EN 1993-1-1 (2005). Eurocode 3: Design of steel structures — Part 1-1: General rules and rules for buildings. *CEN.*
[5]. EN 1993-1-3 (2006). Eurocode 3: Design of steel structures — Part 1-3: General rules-Supplementary rules for cold formed members and sheeting. *CEN.*
[6]. EN 1993-1-6 (2007). Eurocode 3: Design of steel structures — Part 1-6: Strength and stability of shell structures. *CEN.*
[7]. EN 10210-2 (2006). Hot finished structural hollow sections of non-alloy and fine grain steels — Part 2: Tolerances, dimensions and sectional properties. *CEN.*